Gas chromatography-mass spectrometry and scanning electron microscopy with energy-dispersive radiograph analysis of biodeteriorative metabolites produced by *Aspergillus* species

Marwa O. Elnahas[a], Donia H. Sheir[a], Osama Amer[b], Ali M. El Hagrassi[c]

Departments of [a]Chemistry of Natural and Microbial Products, [c]Phytochemistry and Plant Systematic, National Research Centre, Giza, [b]Department of Conservation, Faculty of Archeology, Cairo University, Cairo, Egypt

Correspondence to Donia H. Sheir, PhD, Department of Chemistry of Natural and Microbial Products, Pharmaceutical Industries Researches Division, National Research Centre, El Buhouth Street, Dokki 12622, Giza, Egypt. Tel: (+20)1092742474; fax: (+20) 233387 758; e-mail: donia_sheir@yahoo.com

Received: 16 July 2022
Revised: 3 August 2022
Accepted: 9 August 2022
Published: xx Month 2022

Egyptian Pharmaceutical Journal 2022, 21:482–495

Background and objectives
Fungal deterioration of cultural heritage is a major problem that causes physical and chemical damage as well as esthetic alteration. In the current research, fungal species that exist on a brick sample obtained from Egyptian historical places were isolated and identified. Moreover, various metabolic products produced by the isolated fungal species were detected, which may play an important role in the deterioration of many historical buildings.

Materials and methods
Various fungi existing on brick samples collected from an Egyptian historical place were identified phenotypically and then confirmed molecularly based on the 18 S rDNA technique. The metabolites found in the chloroform extract of the isolated fungi were detected by gas chromatography-mass spectrometry. Quantitative mineralogical analysis of the deteriorated brick was studied by radiograph diffraction. Moreover, scanning electron microscopy-energy-dispersive radiograph was employed to identify the mineral compositions and surface structural morphology of the collected brick sample.

Results and conclusion
Three fungi showed the highest occurrence and were identified as *Aspergillus niger*, *Aspergillus terreus*, and *Aspergillus flavus*. The metabolites found in the chloroform extract of the three fungi were detected by gas chromatography-mass spectrometry, which showed that 5-octadecene, (E) was common among *A. niger*, *A. terreus*, and *A. flavus*; nonadecane and E-15-heptadecenal were common between *A. niger* and *A. flavus*; α-cadinol, tetradecane, and hexadecane were common between *A. niger* and *A. terreus*; and trans-caryophyllene, α-humulene, tau-muurolol, and octadecane were common between *A. terreus* and *A. flavus.* In addition, there was a presence of other hydrocarbons and various organic acid esters that play a vital role in the brick deterioration. Moreover, radiograph diffraction and scanning electron microscopy-energy-dispersive radiograph results showed that the brick sample contains Si, Fe, Ca, and Al, with small amounts of Na, Mg, and Cl. The fungal hyphae penetrating the brick sample were also detected. Our results demonstrate that fungi existence could result in physical deterioration by extending their hyphae through the brick pores resulting in stress. Fungi could also lead to chemical deterioration due to the production of different acids and acid derivatives that cause the brick demineralization via chelation of various metal. In addition, the production of various aliphatic and aromatic hydrocarbons by the fungi could play an important role in the deterioration process.

Keywords:
Aspergillus species, brick-masonry, fungal deterioration, hydrocarbon, organic acid derivatives

Egypt Pharmaceut J 21:482–495

1687-4315

Introduction

Masonry has been used in the construction of the most long-lasting exciting ancient monuments and is present in the most impressive historical structures as evidence of the spirit of enterprise of ancient cultures. Moreover, bricks are one of the oldest man-made building materials starting from sundried clay bricks to the fire bricks, which are fired by clay, calcium-silicate, or concrete to produce hard weather-resistant material to be used for construction [1,2]. The earliest bricks were shaped by wooden brick moulds, and bricks were produced from an extruded pug. A rotating wire was used to cut them to length. Some bricks were underfired and were not as durable, and others might be overfired or overvitrified and might be

distorted; these were discarded or crushed to make 'grog' [3].

The technology of producing and using red-bricks as a construction material in the architectural heritage in Egypt started in ancient times; thus, the Egyptian builders efficiently used brick-masonry in the construction of various building elements such as walls, arches, vaults, domes, and even as a filling material for the construction of multileaf stone-masonry walls. In general, the brick-masonry elements were generally built of red-bricks bonded with lime-based mortar in their joints with different texture systems (Fig. 1). The mortar was used to hold the masonry units together and compensate for their dimensional tolerances. Another purpose for the mortar is to transfer the gravitational force uniformly through the brickwork, the tying effect being achieved by friction and the staggered pattern of the bricks [4,5]. Additionally, bricks can be characterized through the physical-chemical composition of the raw materials and the production issues, such as the firing temperature [6].

Building surfaces are greatly affected by various deterioration factors, including weathering, organic and inorganic matter, black carbon deposition, as well as microbiological growth [7]. These different factors can lead to serious chemical, physical, and biological deterioration of building surfaces, including the historical ones, which in turn affect the cultural heritage [8]. The last decades showed a dramatic increase in the nonbiological weathering processes especially in urban areas, owing to the strong effect of environmental pollution [9,10]. These damaging effects on buildings including monuments are well reported [11,12]. Besides these nonbiological harmful factors, it was found that biological factors play an important role in accelerating the deterioration of the outdoor material. Many metabolic molecules including organic acids as well as polysaccharides (that form biofilms) are produced by these microbial communities, and these bioproducts contribute to the deterioration process [10]. Many growing microbial communities exit on the building materials and form biofilms [13]. These biofilms may contain cyanobacteria, algae, bacteria, fungi, lichens, as well as some plants such as bryophytes, and also it may have small animals such as arthropods [14]. Many factors affect biological growth, including external factors and the intrinsic properties of the building materials [10,15,16]. Temperature, sunlight, wind, and moisture are among the most important external conditions that extensively affect microbial metabolism.

Figure 1

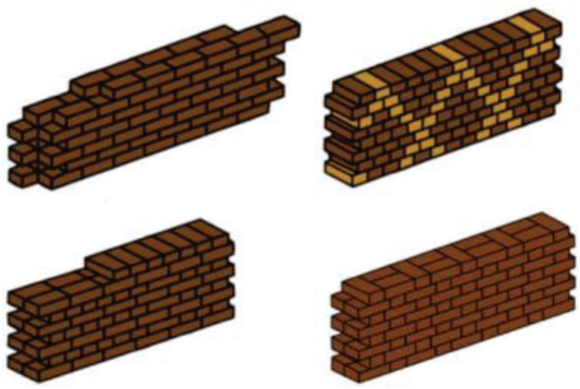

Common running bonds of brick-masonry walls: stretcher (up, left), header (up, right), English (down, left), and Flemish (down, right) bonds [3].

The wet building facade particularly in rainy regions provides a suitable environment for microbial growth, thus enhancing biofouling [17]. Moreover, high temperatures and wind help water to evaporate from these materials. Taken together, all these climatic factors will influence biogrowth [18]. For example, the occurrence of moisture in enough amount together with suitable temperatures leads to a quick biogrowth even on new buildings [19]. On the contrary, biological development is also influenced by the building materials' intrinsic characteristics, which are also defined as their bioreceptivity [14,20]. Primary bioreceptivity means that the building materials have not been exposed to any colonization yet, and their properties remain the same as or very similar to their beginning states. Over time and with the effect of colonizing organisms as well as many other factors, a new form of bioreceptivity is developed and known as secondary bioreceptivity. Additionally, tertiary bioreceptivity can also be induced by human activity that influences these materials, such as surface polishing or coating with biocides [21]. Buildings material colonization by various organisms results in physical damage to the buildings' structures. Microorganisms will get their nutrients and other important elements through the biosolubilization of the substratum. This process involves the production of various substances by the microorganisms including organic and inorganic acids as well as some chelating agents [8,15]. This results in both chemical corrosion of buildings structures as well as physical degradation that are induced by microbial growth [7,22].

Among these microorganisms are fungi. Being heterotrophic organisms, fungi show their ability to grow in the presence of organic nutrient sources. Fungi

can degrade and metabolize the organic matters that are produced by phototrophic organisms and thus resulting in stone decaying and discoloration via the release of various acidic metabolites (mainly organic acids) [23]. It was reported that buildings' organic materials (chemically polluted) supply nutrition sources for heterotrophic organisms [11,24]. The adsorbed pollutants are mainly formed of organic materials such as fatty acids as well as aromatic and aliphatic hydrocarbons, and these, in turn, lead to both chemical and esthetical modifications of the buildings' surfaces nature [25]. Fungi rarely exist on stones as the major biomass; however, they are commonly found on paints or other substrates like bricks. The fungi need enough amounts of moisture together with organic substances to grow. The moister contents help various nutrients to diffuse into the fungal cells, which in turn help in the production of different enzymes, organic and inorganic acids [8,26]. Few studies have been done on the fungal community biodiversity on the surfaces. Nevertheless, some studies revealed some of the main taxa that exist on some rock monuments as well as other painted surfaces such as *Alternaria*, *Aspergillus*, *Aureobasidium*, *Penicillium*, *Phialophora*, *Phoma*, *Sarcinomyces*, as well as others [27–29]. It was also reported that the biodiversity of the fungi is much higher in the urban area compared with rural ones, and this might return mainly to the high organic pollution levels found in the cities [28,30]. Some studies reported the biodegradation that resulted from fungal growth associated with the wood and soils in an archeological site located in Upper Egypt [31]. This study showed that the isolated fungi can colonize wood resulting in biomass loss.

In the current research, we isolated and identified the fungal species that exist on a brick sample obtained from an Egyptian historical place known as The Takiyya of Ibrahim al-Gulshani. The Takiyya of Ibrahim al-Gulshani, also known as the Takiyyat Al-Kulshaniyya, is located at the western side of Taht al-Rab' street nearby Bab Zuwaila and Al-Mu'ayyad mosque in historic Cairo. Additionally, this study focused on the detection of various metabolic products produced by the isolated fungal species that might play an important role in the deterioration of various historical buildings. This will help to develop safer and more effective control techniques to protect and save many heritage buildings.

Materials and methods

Isolation of fungal strains from deteriorated brick-masonry

Brick-masonry samples were collected from the Takiyya of *Ibrahim al-Gulshani*, located at the western side of Taht al-Rab' street nearby Bab Zuwaila and Al-Mu'ayyad Mosque in historic Cairo, Egypt. The brick sample was collected with a sterile spatula and packed in clean dry and sterile polythene bags, and then samples were transferred immediately to the laboratory for fungi isolation. The fungi were isolated according to the dilution plate technique with some modification [32], where 5 g of the brick sample was diluted in 50 ml of potato dextrose broth (PDB) medium (Thermo Fisher Scientific, Fair Lawn, New Jersey, USA). Overall, 100 µg of chloramphenicol was added as an antibacterial agent to minimize any bacterial growth. The medium with the brick sample was placed in a shaker at 100 rpm for 120 min and 30°C. Serial dilutions of the inoculated medium were prepared in sterile saline solutions 0.85% (w/v) NaCl, with a final volume of 10 ml of three different dilutions (10^{-1}, 10^{-2}, and 10^{-3}). The diluted solution was then spread over potato dextrose agar (PDA) plate containing chloramphenicol with a sterile hockey stick. Finally, the PDA plates were incubated at room temperature (28°C) for 7 days. The colony of fungi that appeared in the plate after incubation was then isolated in a new PDA plate. The subculturing step was repeated till a pure culture of each colony was obtained on each plate. The isolated fungal colonies were morphologically identified and finally preserved and kept at −20°C in glycerol 20% (v/v).

Molecular confirmation of the isolated fungus from deteriorated brick-masonry

One of the isolated fungi that showed the highest occurrence was selected and identified based on 18 S rDNA. Overall, 2 ml of 48 h fungal culture grown in PDB medium was used for DNA extraction. The fungus DNA was extracted and purified through E. Z.N.A. Fungal DNA Mini Kit (D3390-01; Omega BIO-TEK, Inc., Doraville, GA, USA) according to the manufacturer protocol. The PCR amplification of 18 S rDNA was carried out with DreamTaq Green PCR Master Mix (2X) (K1081, Thermo Fisher) PCR system cycler where general eukaryotic 5′ and 3′ 18 S rRNA primers 5′-CCTGGT TGATCCTGCC AGTA-3′ and 5′-GCTTGATCCTTCTGCA GGTT-3′ were employed [33]. The results are presented in Fig. 2.

Taxonomic identification of isolated fungi was accomplished using the phenotypic approach down to the species level based on the identification key for *Aspergillus* species by Abdel-Azeem *et al.* [34]. The names of authors of fungal taxa are abbreviated according to Kirk and Ansell (1992).

Figure 2

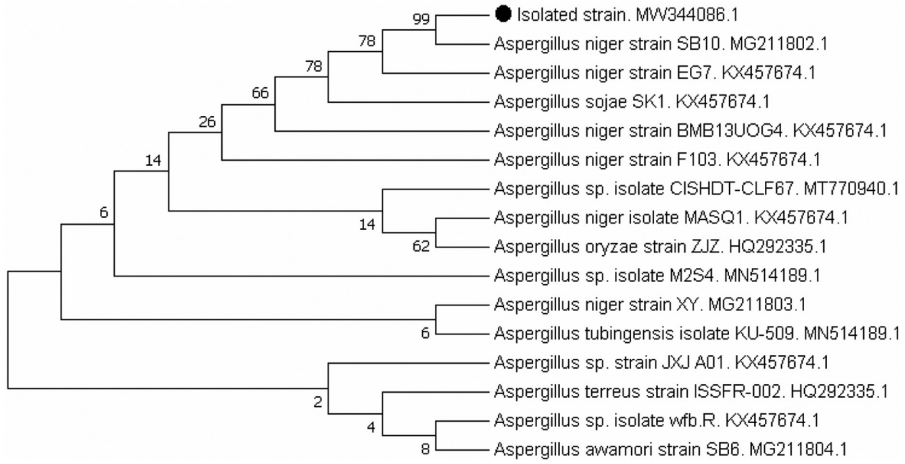

Maximum likelihood phylogenetic tree of the isolated fungal strain based on 18 S rRNA gene sequencing of a 1639 base pair fragment.

Extraction and gas chromatography-mass spectrometry analysis of the secondary metabolites of the fungal strains

Each fungal isolate was inoculated in 250-ml Erlenmeyer flasks containing 50 ml of autoclaved PDB and shaken at 120 rpm at 28°C for 5 days. Chloroform was used for the extraction of active metabolites produced in the PDB medium. After extraction, the extracts were evaporated until dry under reduced pressure and 35°C.

A gas chromatography-mass spectrometry (GC-MS) instrument (TRACE GC Ultra Gas Chromatographs; THERMO Scientific Corp., Waltham, Massachusetts, USA), coupled with a THERMO mass spectrometer detector (ISQ_Single Quadrupole Mass Spectrometer, ThermoScientific, San Jose, California, USA), was employed for the detection of the metabolites. The GC-MS system was equipped with a TG-WAX MS column (30 m×0.25 mm daily, 0.25-µm film thickness). The analysis was carried out using helium as a carrier gas at a flow rate of 1.0 ml/min and a split ratio of 1 : 10 using the following temperature program: 60°C for 1 min, rising at 3.0°C/min to 240°C, and held for 1 min. The injector and the detector were held at 240°C. Diluted samples (1 : 10 chloroform, v/v) of 0.2 µl of the mixtures were always injected automatically in the splitless mode. Mass spectra were obtained by electron ionization at 70 eV, using a spectral range of m/z 40–450. Most of the compounds were identified using the analytical method: mass spectra (authentic chemicals, Wiley spectral library collection, and NSIT library). The quantification of the components was based on the metabolites as detected by the mass spectrometer. Identification of the constituents was carried out by comparison of their retention times and fragmentation pattern of mass with those of published data [35], and/or with those of the Wiley 9 and NIST08 mass spectral libraries.

Quantitative mineralogical analysis of deteriorated brick-masonry by radiograph diffraction

Radiograph diffraction (XRD) was employed to identify the mineral compositions of the collected brick sample. The tested brick sample was prepared for analysis, dried at 110°C, and grounded to a size less than 75 mm. In the current study, PAN analytical XRD equipment model X×^{3}Pert PRO with secondary monochromator was employed. The analysis was conducted with Ni-filter and Cu-Kα radiation (λ=1.542 Å) at 45 KV., 35 MA, and a scanning speed 0.02° (2θ)/s). The scan was collected in a range between 0 and 60°2θ, corresponding spacing (d, Å), and relative intensities (I/I°). Then, the obtained diffraction charts and relative intensities were compared with the data available at the International Centre for Diffraction Data (ICDD files). The XRD charts of the output results are shown in Fig. 5.

Scanning electron microscopy-energy-dispersive radiograph analysis of the deteriorated brick-masonry

The surface structural morphology, as well as elemental composition of the brick sample, was investigated through scanning electron microscopy with energy-dispersive radiograph (EDX) detector. This helps determine the existence of minerals and voids as well as determine weathering status. In the current study, SEM Model Quanta 250 Field Emission Gun (USA) attached with EDX Unit (Energy Dispersive X-ray Analyses), with accelerating voltage 30 kV,

magnification 14× up to 1 000 000×, was employed. Qualitative analysis using EDX was performed on uncoated samples to avoid overlap of gold peaks with peaks of interest [36,37], with a higher accelerating voltage of 20 kV and a large spot size than the imaging. The resolution for Gun.1n. EDX spectra was recorded in the spot-profile mode by focusing the electron beam onto specific regions of the sample, and EDX spectra were obtained between 0 to 10 KeV.

Results and discussion

Fungi

Three fungal strains were the most abundant in deteriorated samples: *Aspergillus niger*, *Aspergillus terreus*, and *Aspergillus flavus* (Table 1). However, *A. niger* was the most abundant isolate, and its identity was further confirmed by using the 18 S rDNA sequence technique. A 1639-base pair fragment of the 18 S rDNA of the isolate was sequenced, and the genus of the isolated fungus was assigned with a maximum likelihood phylogenetic tree and sequence alignment (Fig. 2). The isolated fungal strain shows high sequence identity (>99%) to that *A. niger strain* SB10. The 18 S rDNA sequence has been submitted to GenBank with accession number MW344086.1, (available at https://www.ncbi.nlm.nih.gov/nuccore/MW344086.1).

These results are in agreement with those reported by De Souza and Matoski [38], who also isolated filamentous fungi of the *Aspergillus* genre (*A. niger and A. flavus*) from brick samples collected from surface walls of a hospital found in Brazil. Moreover, *Aspergillus* species were already reported to be the main deteriorative agents in many historic cultural heritages and stone monuments [39]. It was also observed that fungi grow fast on surfaces that have calcium, like in the concrete case, and this stimulates the fungal organic acid production [40,41].

Gas chromatography-mass spectrometry analysis of the secondary metabolites of the fungal strains

To determine the various metabolites found in chloroform extract of the isolated fungal strains, GC/MS analysis was conducted. The identification of these metabolites could help in managing the process of brick deterioration. GC-MS analysis was performed on the chloroform extract of the PDB medium cultivated separately with the three isolated fungi. All the results of the three fungal extracts were accomplished using computer search user-generated reference libraries, incorporating mass spectra. Peaks were examined by single-ion chromatographic reconstruction to confirm their homogeneity. In some cases, when identical spectra have not been found, only the structural type of the corresponding component was proposed based on its mass spectral fragmentation. Reference compounds were co-chromatographed when possible, to confirm GC retention times. Of 60 metabolites detected in the strains belonging to the *Aspergillus* species, 10 metabolites were common between two or three species as follows: only 5-octadecene, (E) was common among *A. niger*, *A. terreus,* and *A. flavus*;; α-cadinol, tetradecane, and hexadecane are common between *A. niger* and *A. terreus*; trans-caryophyllene, α-humulene, tau-muurolol, and octadecane were common between *A. terreus* and *A. flavus*; and finally, nonadecene and E-15-heptadecenal were common between *A. niger* and *A. flavus* (Table 2).

Metabolites obtained from chloroform extract of *Aspergillus niger*

GC-MS analysis was performed on the chloroform extract of the PDB medium cultivated with the three isolated fungi. All the results of the three fungal extracts were accomplished using computer search user-generated reference libraries, incorporating mass spectra. Peaks were examined by single-ion chromatographic reconstruction to confirm their homogeneity. In some cases, when identical spectra have not been found, only the structural type of the corresponding component was proposed based on its mass spectral fragmentation. Reference compounds were co-chromatographed when possible, to confirm GC retention times.

For the *A. niger* chloroform extract, the results revealed the presence of 27 compounds (Fig. 3a). The total peak areas of the detected compounds are 100%, and the probabilities of the structures of the detected compounds are listed in Table 1. The major

Table 1 Fungal isolates and their percentages of occurrence

Fungi	Frequency of occurrence			Color of fungal colonies
	Sample 1	Sample 2	Sample 3	
Aspergillus niger	80%	90%	85%	Dark brown to black colonies
Aspergillus flavus	10%	5%	5%	Green colonies
Aspergillus terreus	10%	5%	15%	Brownish colonies that get darker as they age

Table 2 Secondary metabolites produced by the selected fungal species

Metabolite	M.wt	MF	*Aspergillus niger*			*Aspergillus terreus*			*Aspergillus flavus*		
				R_t (min)	Area%		R_t (min)	Area%		R_t (min)	Area %
methyl(1-methylethyl), Benzene	134	$C_{10}H_{14}$				×	9.22	3.26			
1-Ethylidene-2,2-dimethyl-3-methylenecyclopentane	136	$C_{10}H_{16}$				×	9.97	2.13			
Tricyclene	136	$C_{10}H_{16}$							×	10.26	0.49
2,7-dimethyl-, (E), 3-Octen-5-yne	136	$C_{10}H_{16}$				×	10.19	4.55			
(3-methylbutyl), Cyclopentane	140	$C_{10}H_{20}$	×	17.57	0.26						
1-Decene	140	$C_{10}H_{20}$				×	13.92	2.02			
1- (Hydroxyphenyl)-2-methylpropane	150	$C_{10}H_{14}O$				×	17.25	1.82			
L-Fenchone	152	$C_{10}H_{16}O$				×	11.05	1.09			
4,5-dimethyl, Nonane,	156	$C_{11}H_{24}$	×	14.14	2.11						
1-butyl-2-pentyl-, trans,Cyclopropane	168	$C_{12}H_{24}$							×	19.2	8.27
1-Tridecene	182	$C_{13}H_{26}$	×	19.21	8.35						
Tetradecene	196	$C_{14}H_{28}$							×	23.97	13.14
6,6,6-Trifluoro-5-hydroxy-2,2-dimeth-yl-3-hexanone	198	$C_8H_{13}F_3O_2$	×	5.27	0.27						
Tetradecane	198	$C_{14}H_{30}$	×	19.40	2.77	×	19.40	1.44			
2-Ethylhexyl ester of butanoic acid	200	$C_{12}H_24O_2$				×	8.47	0.63			
α-Copaene	204	$C_{15}H_{24}$				×	18.88	2.26			
trans-Caryophyllene	204	$C_{15}H_{24}$				×	19.99	2.92	×	20.00	0.52
α-Humulene	204	$C_{15}H_{24}$				×	20.83	3.97	×	20.85	0.69
Germacrene D	204	$C_{15}H_{24}$				×	21.52	1.76			
Bicycloelemene	204	$C_{15}H_{24}$				×	21.91	0.67			
ë-Cadinene	204	$C_{15}H_{24}$				×	22.53	3.84			
Calarene	204	$C_{15}H_{24}$							×	22.54	1.05
2-Allyl-5-t-butylhydroquinone	206	$C_{13}H_{18}O_2$				×	22.41	8.15			
2-tert-Butyl-4-isopropyl-5-methylphen-ol	206	$C_{14}H_{22}O$							×	22.41	11.40
Pentadecane	212	$C_{15}H_{32}$							×	19.40	2.39
tau.-Muurolol	222	$C_{15}H_{26}O$				×	25.29	1.40	×	25.29	2.56
α-Cadinol	222	$C_{15}H_{26}O$	×	25.59	0.37	×	25.56	3.11			
6-epi-shyobunol	222	$C_{15}H_{26}O$				×	26.37	2.42			
7-Hexadecene, (Z)	224	$C_{16}H_{32}$				×	23.97	9.40			
3-Hexadecene, (Z)-	224	$C_{16}H_{32}$				×	35.75	5.74			
1-Hexadecene	224	$C_{16}H_{32}$	×	23.97	13.91						
Hexadecane	226	$C_{16}H_{34}$	×	24.14	2.73	×	24.13	1.72			
(1à,4à,4aà,10aà)-1,4,4a,5,6,7,8,9,10,10a-decahydro-1,4,11, 11-tetramethyl-1,4-methanocycloocta[d]pyridazine	234	$C_{15}H_{26}N_2$	×	22.42	10.97						
Heptadecane	240	$C_{17}H_{36}$	×	35.84	1.31						
5-Octadecene, (E)	252	$C_{18}H_{36}$	×	28.28	24.76	×	32.18	9.16	×	32.18	13.14

(*Continued*)

Table 2 (*Continued*)

Metabolite	M.wt	MF	*Aspergillus niger*			*Aspergillus terreus*			*Aspergillus flavus*		
				R_t (min)	Area%		R_t (min)	Area%		R_t (min)	Area %
E-15-Heptadecenal	252	$C_{17}H_{32}O$	×	32.18	13.88				×	28.28	15.38
2,2,4,9,11,11-Hexamethyl, dodecane	254	$C_{18}H_{38}$				×	28.41	2.56			
Octadecane	254	$C_{18}H_{38}$				×	32.29	1.33	×	28.41	2.66
1-Nonadecene	266	$C_{19}H_{38}$	×	39.04	4.17				×	35.75	8.2
cis-2-Nonadecene	266	$C_{19}H_{38}$				×	28.27	10.61			
9-Acetoxy-1-methyl-8-propyl-3,6-diaz-ahomoadamantane	266	$C_{15}H_{26}N_2O_2$	×	53.30	0.28						
Nonadecane	268	$C_{19}H_{40}$	×	28.41	2.67				×	35.84	1.21
Butyric acid, 3-tridecyl ester	270	$C_{17}H_{34}O_2$	×	17.57	0.26						
5-(5-Hexenyl)-3-(8-nonenyl) isoxazole	275	$C_{18}H_{29}NO$				×	19.20	6.21			
7,9-di-tert-butyl-1-oxaspiro[4.5]deca-6,9-diene-2,8-dione	276	$C_{17}H_{24}O_3$	×	30.99	0.61						
3-Trifluoroacetoxydodecane	282	$C_{14}H_{25}F_3O_2$	×	8.48	1.23						
2,6,10,14-tetramethyl, Hexadecane,	282	$C_{20}H_{42}$	×	26.34	0.76						
n-Nonadecanol-1	284	$C_{19}H_{40}O$				×	39.03	2.87			
2,6,10,14-tetramethyl, Heptadecane,	296	$C_{21}H_{44}$	×	32.29	2.37						
1-Eicosanol	298	$C_{20}H_{42}O$	×	42.09	1.23						
Docosane	310	$C_{22}H_{46}$				×	35.84	1.31			
Trichloroacetic acid,pe-ntadecyl ester	372	$C17_7H_{31}C_{l3}O_2$									
1,2-Benzenedicarboxylicacid, bis(2-ethylhexyl) ester	390	$C_{24}H_{38}O_4$	×	41.60	0.23						
2-(3-(1-Hydroxy-1-methyl-ethyl)-6a,10b-dimethyl-7-methylene-dodecahydro-benzo[f]chromen-8-yl]-1-phenyl-ethanone	410	$C_{27}H_{38}O_3$	×	48.39	0.67						
Acetic acid,17-acetoxy-4,4,10,13-tetramethyl-7-oxo-2,3,4,7,8,9,10,11,12, 13,14,15,16,17-tetradecahydro-1H-cyclopenta[a]phenanthren-3-yl(ester)	416	$C_{25}H_{36}O_5$	×	53.09	0.23						
Ethyl iso-allocholate	436	$C_{26}H_{44}O_5$							×	40.67	0.38
Stearic acid,3- (octadecyloxy) propyl ester	594	$C_{39}H_{78}O_3$	×	53.40	0.33						
Lucenin 2	610	$C_{27}H_{30}O_{16}$	×	44.94	0.29						
ë-Methyl-2-(2-hydroxyethyl)-2-deviny-lchlorin e6 – trimethyl ester	670	$C_{38}H_{46}N_4O_7$							×	30.85	0.36
(5,10,15,20-tetraphenyl [2-(2)H1] prophyrinato) zinc (II)	676	$C_{44}H_{27}DN_4Zn$	×	6.45	0.27						

MF, molecular formula; MW, molecular Weight; R_t, retention time. *X=positive to metabolite production.

Figure 3

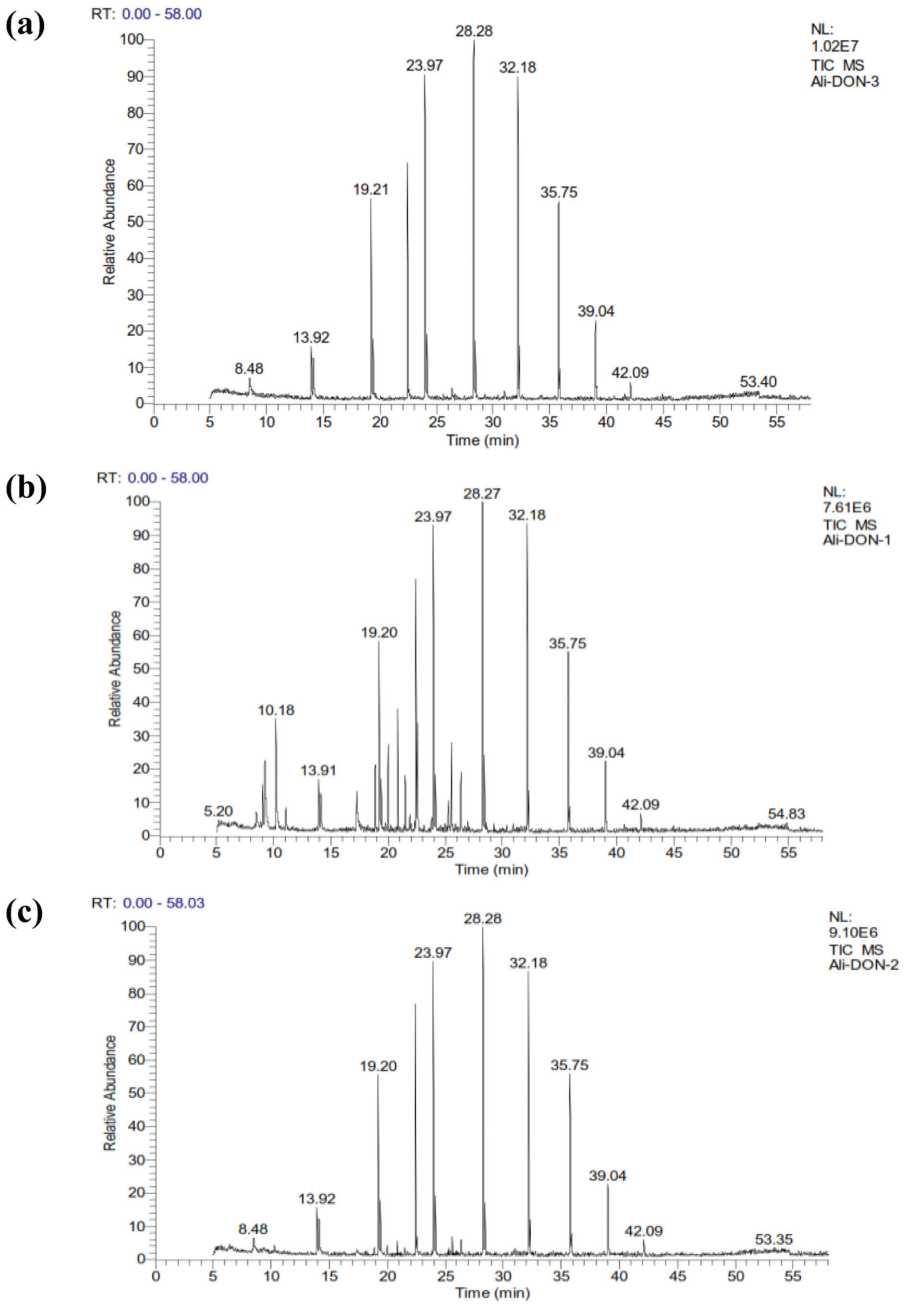

GC/MS analysis of different metabolites detected in the chloroform extracts of (a) *Aspergillus niger*, (b) *Aspergillus terreus*, (c) *Aspergillus flavus*. GC/MS, gas chromatography-mass spectrometry.

compounds are 1-tridecene (8.35%), (1à,4à,4aà,10aà)-1,4,4a,5,6,7,8,9,10,10a-decahydro-1,4,11,11-tetramethyl-1,4-methanocycloocta[d]pyridazine (10.97%), 1-hexadecene (13.91%), 5-octadecene, (E) (24.76%), and E-15-heptadecenal (13.88%), for which represented 71.87% of the total peak areas. Moreover, some organic acid derivatives were also detected, such as acetic acid ester and butyric acid ester. However, acetic acid ester (17-(Acetyloxy)-4,4-dimethyl-7-oxoandrost-5-en-3-yl acetate) and butyric acid ester were detected in the metabolites of *A. niger*. The production of acetic acid could be attributed to the hydrolysis of acetyl group esters, and the rate of hydrolysis depends on the availability of water and the temperature of the environment surrounding it [42].

Metabolites obtained from chloroform extract of *Aspergillus terreus*

GC-MS analysis was also performed on the chloroform extract of the liquid media cultivated with *A. terreus*, and it revealed the presence of 28 compounds (Fig. 3b). The total peak areas of the detected compounds are 100% and the probabilities

of the structures of the detected compounds are listed in Table 1. The major compounds detected in the chloroform extract are cis-2-nonadecene (10.61%), 5-octadecene, (E) (9.16%), 7-hexadecene, (Z) (9.40%), and 2-allyl-5-t-butylhydroquinone (8.15%). Moreover, esters of some acids such as 2-ethylhexyl ester of butanoic acid, and trichloroacetic acid, pentadecyl ester were detected.

Metabolites obtained from chloroform extract of *Aspergillus flavus*

GC-MS analysis was performed on the chloroform extract of the liquid media cultivated with *A. flavus,* and it consisted of 16 compounds (Fig. 3c). The total peak areas of the detected compounds are 100%, and the probabilities of the structures of the detected compounds are listed in the Table 1. The major compounds are 1-butyl-2-pentyl-, trans, cyclopropane, (8.27%), 5-octadecene, (E) (13.14%), E-15-heptadecenal (15.38%), tetradecene (13.14%) and 2-tert-Butyl-4-isopropyl-5-methylphenol (11.40%), for which represented 61.33% of the total peak areas. The identification was accomplished using computer search user-generated reference libraries, incorporating mass spectra. Peaks were examined by single-ion chromatographic reconstruction to confirm their homogeneity. Major secondary metabolites found in the chloroform extract are shown in Fig. 3c. *Aspergillus* species were already reported to be the main deteriorative agents in many historic cultural heritages and stone monuments [39]. It was also observed that fungi grow fast on surfaces that have calcium, like in the concrete case, and this stimulates the fungal organic acid production [40,41].

Moreover, some studies reported the ability of fungi to produce some chelating agents that resulted in the solubilization of the divalent and trivalent cations [11,30]. This chelation process could result in the exfoliation of many monument and historical buildings surfaces [43]. The fungal growth in the bricks causes cracks and crevices on the surfaces due to the production of acids and other organic and inorganic compounds [27]. The organic acids and their derivatives result in the demineralization of several substrates. In conclusion, fungus resulted in coloration, exfoliation, and pitting of historic buildings. The GC/MS analysis obtained from chloroform extract of the isolated fungi also showed the presence of high amounts of various aliphatic and aromatic hydrocarbons such as hexadecene, hexadecane, E-15-heptadecenal, 2-tert-butyl-4-isopropyl-5-methylphenol, tetradecane, 1-nonadecene, cyclopentane as well as many other hydrocarbons. Limited information is available regarding the effect of various hydrocarbon contaminants on building materials. There are few lines of evidence that hydrocarbons could result in the inhibition of concrete strength in the ground [44]. Many sites have been reported to be contaminated with organic hydrocarbons. Among these contaminants are benzene, toluene, xylene, ethyl benzene, naphthalene, anthracene, phenols, cresol, polyaromatic hydrocarbons, phenoxy acid, as well as others. The hydrocarbons resulted in the staining of many buildings [45]. Taken together, the production of various organic acids derivatives as well as several aromatic and aliphatic hydrocarbons could greatly play an important role in the deterioration of various building materials including brick.

Mineralogical characterization

Quantitative analysis using radiograph diffraction of the deteriorated brick-masonry

In the present study, one of the important nondestructive techniques has been applied to analyze the brick sample, which is XRD. In this technique, the matter atoms scatter radiograph waves, through the atoms' electrons [46]. Then, the radiograph radiation determines a wavelength that is of the order of the usual interatomic spacing which is found in the crystalline solids and hence will determine the crystal domain size as well as the nanomaterials structure. Thus, XRD is considered a unique method applied for the determination of the crystallinity of various compounds [47]. The XRD results illustrated the mineralogical composition of the brick units and confirmed that the tested brick sample is formed mainly of quartz, SiO_2; aluminum, Al_2O_3; and ferric oxides, Fe_2O_3. The obtained XRD results (Fig. 4) in our study showed that the brick sample contains quartz (SiO_2), which is identified by the peak at ~26°.

However, quartz is a common component of limestone, sandstone, and granite as well as many various sedimentary and metamorphic rocks [48–50]. The existence of quartz could be related to the use of sand particles as an additive in the manufacturing of bricks. Another reason for the presence of quartz could be attributed to the elevated temperatures that result in the release of water of carbonization and crystallization of many organic compounds via an exothermic reaction. As a result, the aluminum silicate will dehydrate and form SiO_2 [51]. Iron oxide in the form of hematite (Fe_2O_3) was also detected by a peak at ~33°. These data are supported by the result reported by Milinovic *et al*. [52], who also detected a hematite peak at 33.2° in a seafloor sediment sample.

Figure 4

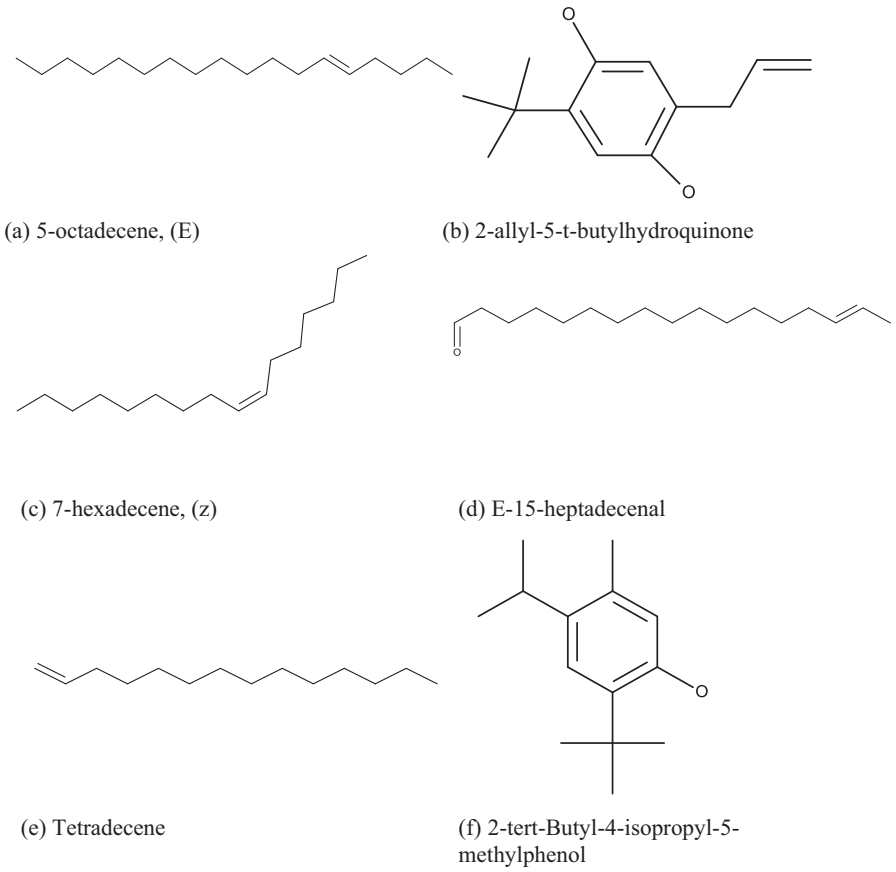

Major compound found in chloroform extract of (a) *Aspergillus niger*, *Aspergillus terreus* and *Aspergillus flavus*, (b, c) *A. terreus*, (d) *Aspergillus niger* and *Aspergillus flavus*, and (e, f) *Aspergillus flavus*.

On the contrary, the mineralogical composition of the mortar sample obtained from the bed-joints of the brick-masonry composes mainly of Calcite-magnesian (Mg.064 Ca.936) (CO_3) together with a high percentage of Quartz SiO_2. Other minor ingredients were also detected including halite (NaCl) and gypsum [$CaSO_4$ $(H_2O)_2$]. It is a lime-based mortar of mainly lime and sand. The existence of clay minerals indicates the addition of homra, in a relatively low percentage to the mortar mixture. Moreover, the presence of halite indicates a slight salt decay infection by chloride salts. Figure 5a and b shows the XRD pattern and the average composition of the minerals of both brick and mortar samples, respectively. Calcite and dolomite are among the most carbonate minerals found in a variety of metamorphic, igneous, and sedimentary rocks [53], and this is obvious in our study, where a peak for magnesium –calcite at ~29.5 is observed in the mortar sample. Sanz-Montero *et al.* [54], also detected a peak for magnesium-calcite at the same range, and this confirms our results. Some minor ingredients were also detected in the XRD of the brick sample such as gypsum, halite, and homra. Gypsum ($CaSO_4 \cdot 2H_2O$) forms in the presence of liquid water, and this helps to identify the surrounding climatic conditions [55]. There is a hypothesis indicating that gypsum development could occur owing to mortar joint carbonation [56]. Gypsum is the stable calcium sulfate form under normal conditions, and this explains its existence in efflorescence; however, gypsum conversion to anhydrite ($CaSO_4$) could occur at elevated temperatures above 350°C [57]. Gypsum efflorescence is a problem that affects brick-masonry. It leads to the development of a thin white film at the surface of the brick and which in turn alters the esthetic features of the valuable construction. Salt efflorescing also resulted from other minerals such as halite (NaCl) that tend to form extensive efflorescence and its accumulation is accompanied by an elevated drying rate, thus sustaining salt growth at the building surface [58]. Moreover, homra was detected in the tested sample. A previous study showed that the

Figure 5

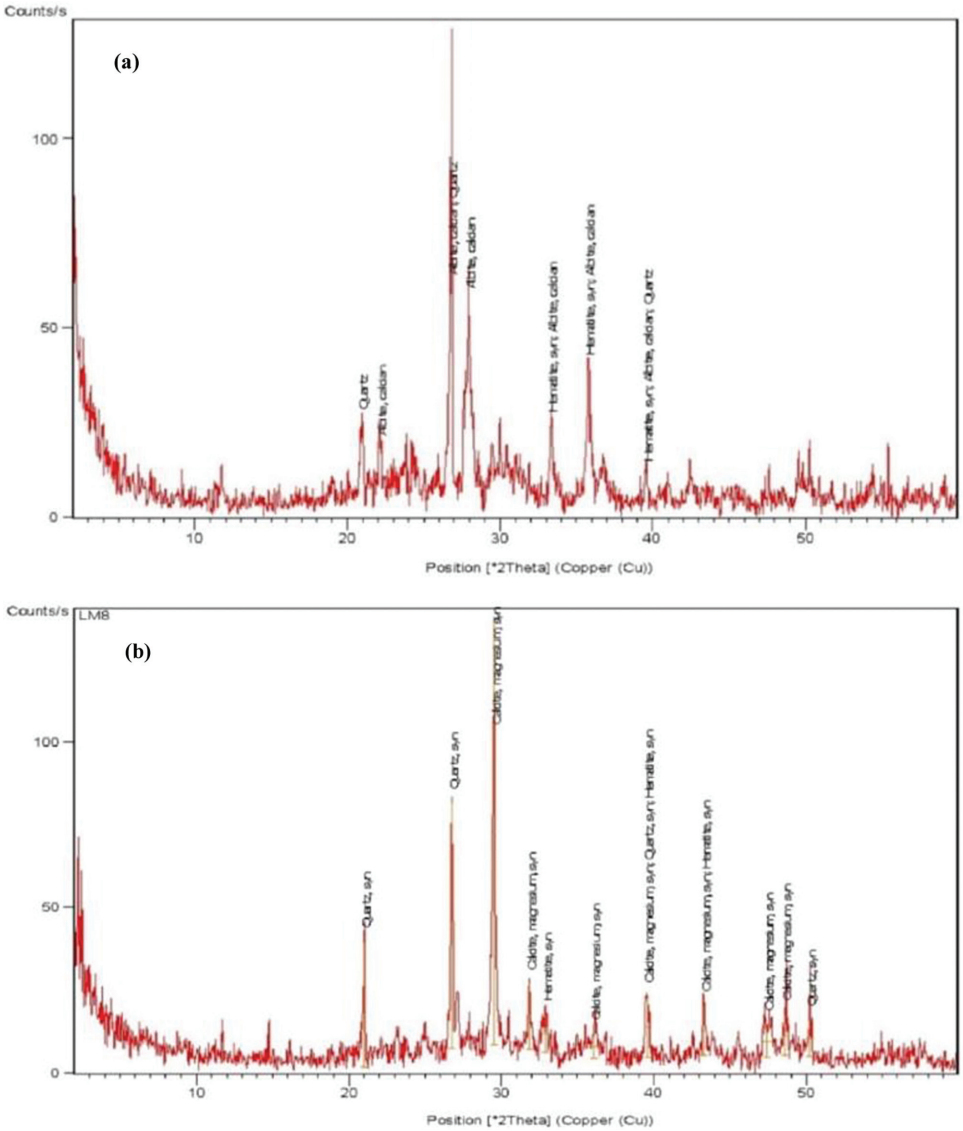

Radiograph diffraction pattern of representative (a) brick and (b) mortar samples.

addition of homra to the other brick components could improve its quality by increasing the brick compressive capacity [59].

Microstructure and micro-morphological examination of brick-masonry by scanning electron microscopy with energy-dispersive radiograph

Scanning electron microscopy (SEM) attached with EDX (microanalysis) was employed to investigate the structural morphology as well as the microstructure of both brick and mortar samples. The scanning showed the presence of pores in the brick sample (Fig. 6a). Moreover, the presence of fungal hyphae was detected (Fig. 6b), that is, SEM-EDX analysis showed a heterogeneous distribution of gaps with the evidence of fungal involvement, where the fungal hyphae penetrate the brick sample (Fig. 6a, b). The porosity of the bricks is a crucial factor that helps the penetration of the fungus. Fungal penetration resulted in a serious physical deterioration of the bricks where hyphal networks will extend through the pore space system of the bricks [60]. Therefore, fungi increase the physical damage of the bricks by extending their hyphae that penetrate into the brick surfaces [61,62] and which consequently result in stresses that damage the brick and the surrounding structures [40].

However, the results of the microscopic examination and elemental analysis of the brick sample showed that the main component of the brick units is quartz, with very fine grains. Heterogeneous distribution of gaps and a minor quantity of crystalline salts (halite, NaCl) through the sample were also detected. EDX analysis

Figure 6

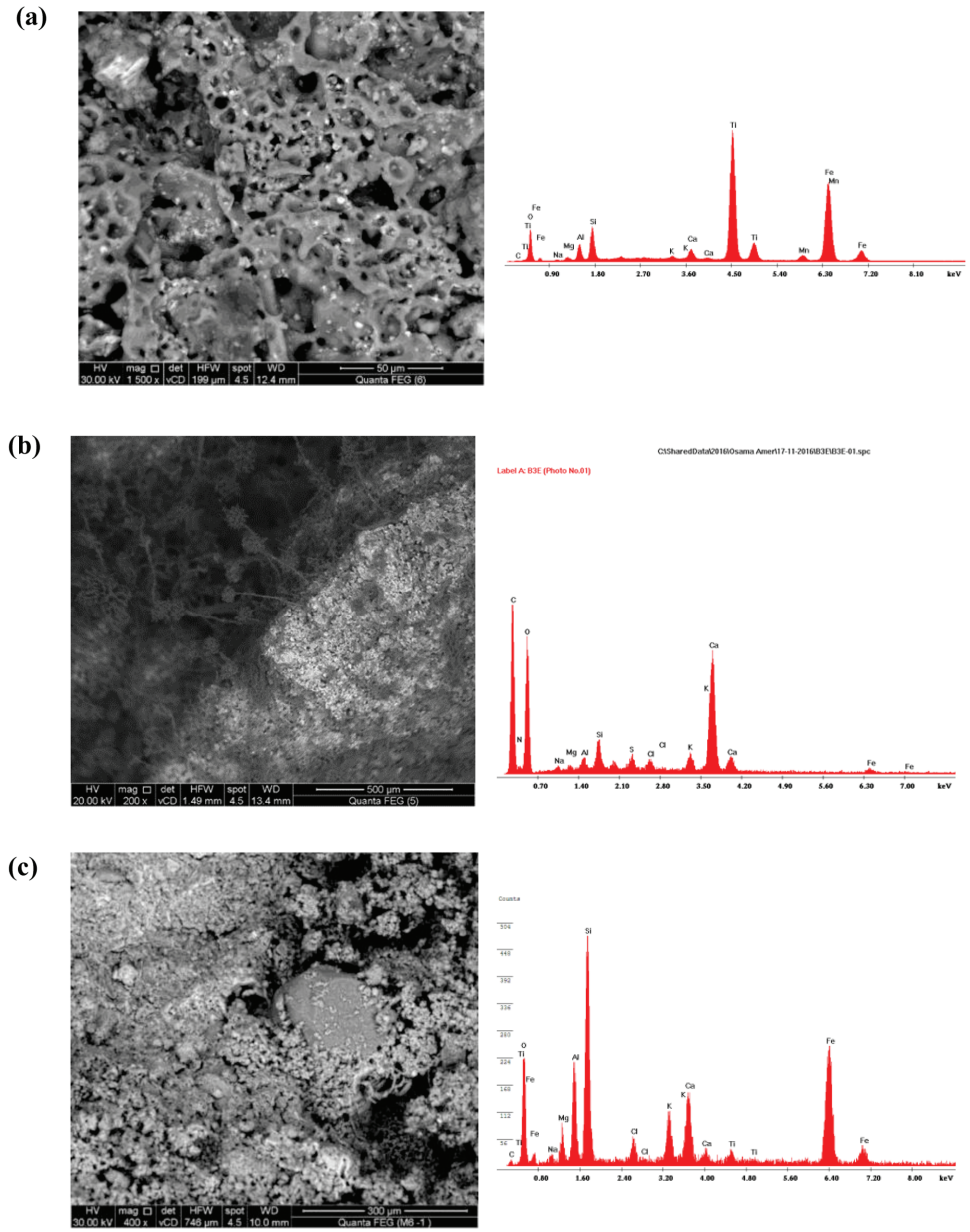

SEM photomicrographs and EDX microanalysis of a thin section of (a) the tested brick showing the occurrence of pores, (b) brick sample showing fungal growth with fungal hyphae, and (c) mortar samples. EDX, energy-dispersive radiograp; SEM, scanning electron microscopy.

showed that the brick sample is enriched in Si, Fe, Ca, and Al with small amounts of Na, Mg, and Cl. Regarding the mortar samples (Fig. 6c), the microscopic examination shows that the mortar is composed mainly of calcite with fine rounded quartz crystals. The quartz grains are also very fine and scattered in the mortar. Moreover, EDX analysis shows that the tested mortar sample is enriched in Fe, Ca, and Si as major elements. However, Cl, Mg, Al, Na, and S are found as minor elements. It is worth remarking that the presence of Ca and Mg confirms the importance of carbonate phases $CaCO_3$, $CaMg(CO_3)_2$, whereas the presence of Na, S, and Cl confirms the infection by chloride and sulfate salt decay (e.g. NaCl and $CaSO_4$). Additionally, the presence of Mg, Al, and Fe confirms that the sample contains clay minerals which confirm the XRD results. Almost all of these elements are found in the building materials of all historical buildings [10,61]. The organic acids produced due to fungal growth lead to the solubilization and/or chelation of minerals such as Ca, A1, Fe, and Ks from the building materials including bricks and mortar [63].

Conclusion

Cultural heritage is greatly affected by various types of deterioration such as physical, chemical, and biological

deterioration. The current study in the field of geomicrobiology has focused on understanding the different roles of fungi in the biodeterioration of valuable historic monuments formed mainly of masonry brick with the aid of various techniques such as XRD, SEM-EDAX, and GC-MS. The present study has tried to figure out a relationship between the occurrence of various fungal strains and their metabolites to the deterioration of historic brick to better comprehend their contribution to the biodeterioration of building materials. Our results demonstrate that fungus existence resulted in the physical deterioration of the monument by extending their hyphae through the brick pores resulting in stress on the brick. Moreover, fungi could result in chemical deterioration due to the production of different acids and acid derivatives that leads the brick demineralization via chelation of various metals [63]. In addition, the production of various aliphatic and aromatic hydrocarbons by the fungi could play a role in the deterioration process. The existence of fungal strains in various monuments resulted in discoloration, pitting, exfoliation, etc. Thus, the identification of the microbial communities that exist on the building is a very important tool that helps control microbial biodeterioration. Various factors that promote microbial growth and survival on the brick surface should also be evaluated to control microbial growth. Understanding the deterioration mechanism caused by different microbes should be well studied to design appropriate conservation and restoration strategies for historic buildings [63]. For future work, various techniques should be employed to get more insight into mechanisms and various causes of deterioration processes. Among these techniques are terminal restriction fragment length polymorphism, laser-induced fluorescence, Mössbauer spectrometry, fourier transform infrared spectroscopy, induction coupled plasma-mass spectrometry, thermal analysis, laser, mercury intrusion porosimetry, high-performance liquid chromatography, etc.

Financial support and sponsorship
Nil.

Conflicts of interest
There are no conflicts of interest.

References

1 Amer O, Abdel-Aty Y, El-Hady MA, Aita D, Torky A, Hussein YM. Multiscientific-based approach to diagnosis and characterization of historic stone-masonry walls: The mausoleum of Al-Imam Al-Shafi'i, Cairo (Egypt). Mediter Archaeol Archaeometry 2020; 20:2.

2 Misra AK. Building materials and construction. New Delhi, India: S Chand & Co. Ltd.,; 2018.

3 Maldonado NG, Martín P, del Solar GG, Domizio M. Historic Masonry, Heritage, IntechOpen 2019. https://www.intechopen.com/chapters/68031

4 Kamendere E, Grava L, Zvaigznitis K, Kamenders A, Blumberga A. Properties of bricks and masonry of historical buildings as a background for safe renovation measures. Energy Proc 2016; 95:119–123.

5 Amer O, Saad B, Karim A. Finite element analyses for seismic performance assessment of historical masonry buildings: the case of Omar Toson palace (Cairo, Egypt). Mediter Archaeol Archaeometry 2017; 17:3.

6 Barluenga G, Estirado F, Undurraga R, Conde JF, Agua F, Villegas MÁ, García Heras M. Brick masonry identification in complex historic buildings, Constr Build Mater 2014; 54:39–46.

7 Sleiman M, Kirchstetter TW, Berdahl P, Gilbert HE, Quelen S, Marlot L, *et al.* Soiling of building envelope surfaces and its effect on solar reflectance-Part II: development of an accelerated aging method for roofing materials, Solar Energy Mater Solar Cells 2014; 122:271–281.

8 Gaylarde C, Morton G. Biodeterioration of mineral materials, Encyclopedia of Environmental Microbiology. In: Bitton G. New York: John Wiley & Sons. 2003. 516–527.

9 Tran TH, Govin A, Guyonnet R, Grosseau P, Lors C, Garcia-Diaz E, *et al.* Influence of the intrinsic characteristics of mortars on biofouling by *Klebsormidium flaccidum*. Int Biodeteriorat Biodegrad 2012; 70:31–39.

10 Tomaselli L, Lamenti G, Bosco M, Tiano P. Biodiversity of photosynthetic micro-organisms dwelling on stone monuments. Int Biodeterior Biodegrad 2000; 46:251–258.

11 Gómez-Alarcón G, Munoz M, Flores M. Excretion of organic acids by fungal strains isolated from decayed sandstone. Int Biodeterior Biodegrad 1994; 34:169–180.

12 Ortega-Calvo J, Hernandez-Marine M, Saiz-Jimenez C. Experimental strategies for investigating algal deterioration of stone. Proceedings of the 7th International Congress on Deterioration and Conservation of Stone: held in Lisbon, Portugal, June 15-18, 1992; 541–549

13 Characklis W. Biofilm processes. In: Characklis WG, Marshall KC, editors. Biofilms. New York: John Wiley & Sons; 1990; p. 195–231.

14 Gaylarde CC, Gaylarde PM. A comparative study of the major microbial biomass of biofilms on exteriors of buildings in Europe and Latin America. Int Biodeterior Biodegrad 2005; 55:131–139.

15 John D. Algal growths on buildings: a general review and methods of treatment. Biodeterior Abstracts 1988; 2(67):81–102.

16 Barberousse H, Lombardo RJ, Tell G, Couté A. Factors involved in the colonisation of building façades by algae and cyanobacteria in France. Biofouling 2006; 22:69–77.

17 Tran TH, Govin A, Guyonnet R, Grosseau P, Lors C, Damidot D, *et al.* Influence of the intrinsic characteristics of mortars on their biofouling by pigmented organisms: Comparison between laboratory and field-scale experiments. Int Biodeterior Biodegrad 2014; 86:334–342.

18 Ariño X, Gomez-Bolea A, Sáiz-Jiménez C. Lichens on ancient mortars. Int Biodeterior Biodegrad 1997; 40:217–224.

19 Wee Y, Lee K. Proliferation of algae on surfaces of buildings in Singapore. Int Biodeterior Bull 1980; 16:113–117.

20 Guillitte O. Bioreceptivity: a new concept for building ecology studies. Sci Total Environ 1995; 167:215–220.

21 Sanmartín P, Miller A, Prieto B, Viles HA. Revisiting and reanalysing the concept of bioreceptivity 25 years on. Sci Total Environ 2021; 770:145314.

22 Gaylarde CC, Morton LG. Deteriogenic biofilms on buildings and their control: a review. Biofouling 1999; 14:59–74.

23 Falkiewicz-Dulik M, Janda K, Wypych G. Handbook of material biodegradation, biodeterioration and biostablization. Toronto, Ontario M1E 1C6, Canada: Elsevier; 2015.

24 Zanardini E, Abbruscato P, Ghedini N, Realini M, Sorlini C. Influence of atmospheric pollutants on the biodeterioration of stone. Int Biodeterior Biodegrad 2000; 45:35–42.

25 Sáiz-Jiménez C. Deposition of anthropogenic compounds on monuments and their effect on airborne microorganisms. Aerobiologia 1995; 11:161–175.

26 Griffin P, Indictor N, Koestler RJ. The biodeterioration of stone: a review of deterioration mechanisms, conservation case histories, and treatment. Int Biodeterior 1991; 28:187–207.

27 Bravery A. Biodeterioration of paint—a state-of-the-art comment. Biodeterioration 7. London, United Kingdom: Springer; 1988. 466–485

28 Sterflinger K, Prillinger H. Molecular taxonomy and biodiversity of rock fungal communities in an urban environment (Vienna, Austria). Antonie Van Leeuwenhoek 2001; 80:275–286.

29 Gu J-D., Ford TE, Berke NS, Mitchell R. Biodeterioration of concrete by the fungus Fusarium. Int Biodeterior Biodegrad 1998; 41:101–109.

30 Shirakawa MA, Gaylarde CC, Gaylarde PM, John V, Gambale W. Fungal colonization and succession on newly painted buildings and the effect of biocide. FEMS Microbiol Ecol 2002; 39:165–173.

31 Abdel-Azeem AM, Held BW, Richards JE, Davis SL, Blanchette RA. Assessment of biodegradation in ancient archaeological wood from the middle cemetery at Abydos, Egypt. PLoS ONE 2019; 14:e0213753.

32 Garrett SD. Soil fungi and soil fertility: An introduction to soil mycology. London, United Kingdom: Elsevier; 2016.

33 Dams E, Hendriks L, Van de Peer Y, Neefs J-M., Smits G, Vandenbempt I, De Wachter R. Compilation of small ribosomal subunit RNA sequences. Nucleic Acids Res 1988; 16 (Suppl):r87.

34 Abdel-Azeem AM, Abu-Elsaoud A, Darwish AMG, Balbool BA, Abo Nouh F, Abo Nahas HH, *et al.* The Egyptian Ascomycota 1: Genus Aspergillus. Microb Biosyst 2020; 5:61–99.

35 Adams RP. Identification of essential oil components by gas chromatography/mass spectrometry. Carol Stream, IL: Allured publishing corporation; 2007.

36 Moropoulou A, Zendri E, Ortiz P, Delegou ET, Ntoutsi I, Balliana E, *et al.* Scanning microscopy techniques as an assessment tool of materials and interventions for the protection of built cultural heritage. Scanning 2019; 2019:5376214.

37 Raw-Rees S, Pesce GL, Ball RJ, Fodde E. Characterization of binders in the historic lime mortars and plasters from 1A Royal Crescent, Bath. J Build Limes Forum 2012; 19:28–37.

38 De Souza WB, Matoski A. Characterization of mould in masonry in hospital environment—case study. Open J Civil Eng 2016; 6:618.

39 Burford E, Fomina M, Gadd G. Fungal involvement in bioweathering and biotransformation of rocks and minerals. Mineral Mag 2003; 67:1127–1155.

40 Beech IB, Gaylarde CC. Microbial polysaccharides and corrosion. Int Biodeterior 1991; 27:95–107.

41 Dutton MV, Evans CS. Oxalate production by fungi: its role in pathogenicity and ecology in the soil environment. Can J Microbiol 1996; 42:881–895.

42 Gibson LT, Watt CM. Acetic and formic acids emitted from wood samples and their effect on selected materials in museum environments. Corrosion Sci 2010; 52;172–178.

43 Warscheid T, Petersen K, Krumbein WE. A rapid method to demonstrate and evaluate microbial activity on decaying sandstone. Stud Conserv 1990; 35:137–147.

44 Wilson S, Langdon N, Walden P. The effects of hydrocarbon contamination on concrete strength. Proce Inst Civil Eng 2001; 149:189–193.

45 Pye P, Harrison H. Floors and flooring: performance, diagnosis, maintenance, repair and the avoidance of defects, bre building elements series. London: Construction Research Communications; 1997.

46 Bowen P. Particle size distribution measurement from millimeters to nanometers and from rods to platelets. J Disp Sci Technol 2002; 23:631–662.

47 Nasrollahzadeh M, Atarod M, Sajjadi M, Sajadi SM, Issaabadi Z. Plant-mediated green synthesis of nanostructures: Mechanisms, characterization, and applications. Interface Science and Technology. London, United Kingdom: Elsevier; 2019. 199–322

48 Lyon R. Infrared absorption spectroscopy. En: Zussman J. (Ed.), Phys Methods Determinat Mineral. London: Academic Press 1967; 371–399.

49 Chester R, Green R. The infra-red determination of quartz in sediments and sedimentary rocks, Chem Geol 1968; 3:199–212.

50 Kaufhold S, Hein M, Dohrmann R, Ufer K. Quantification of the mineralogical composition of clays using FTIR spectroscopy. Vib Spectrosc 2012; 59:29–39.

51 Sheikh MR, Barua AG. X-ray diffraction and Fourier transform infrared spectra of the bricks of the Kamakhya temple. Indian J Pure Appl Phys 2013; 51:745–748.

52 Milinovic J, Dias ÁA, Janeiro AI, Pereira MF, Martins S, Petersen S, Barriga FJ. XRD identification of ore minerals during cruises: refinement of extraction procedure with sodium acetate buffer. Minerals 2020; 10:160.

53 Dos Santos HN, Neumann R, Ávila CA. Mineral quantification with simultaneous refinement of Ca-Mg carbonates non-stoichiometry by X-ray diffraction, Rietveld method. Minerals 2017; 7:164.

54 Sanz-Montero ME, Cabestrero Ó, Sánchez-Román M. Microbial Mg-rich carbonates in an extreme alkaline lake (Las Eras, Central Spain). Front Microbiol 2019; 10:148.

55 Lafuente B, Bishop J, Fenton L, King S, Blake D, Sarrazin P, *et al.* Mineralogical characterization by XRD of gypsum dunes at White Sands National Monument and application to gypsum detection on Mars, Lunar and Planetary Science Conference XLV, The Woodlands, Texas, Abstract, 2014.

56 Chwast J, Todorović J, Janssen H, Elsen J. Gypsum efflorescence on clay brick masonry: field survey and literature study. Constr Build Mater 2015; 85:57–64.

57 Cramer S, Friday O, White R, Sriprutkiat G. Mechanical properties of gypsum board at elevated temperatures, Fire and materials 2003: 8th International Conference, January 2003, San Francisco, CA, USA. London: Interscience Communications Limited, c2003: pages 33–42. 2003.

58 Chwast J, Janssen H, Elsen J. Gypsum efflorescence under laboratory conditions: preliminary study, 3rd International conference of salt weathering of buildings and stone sculptures, Brussels, Belgium, 2014.

59 Abdelmegeed MM. Modified mud bricks for strengthening historic earthen structures: towards sustainable and green restoration. Shedet 2020; 7:263–276.

60 Urzì C. On microbes and art: the role of microbial communities in the degradation and protection of cultural heritage A report on the International Conference on Microbiology and Conservation (ICMC 1999), Florence, 16–19 June 1999 Wiley Online Library, 1999.

61 Warscheid T, Braams J. Biodeterioration of stone: A review. Int Biodeterior Biodegrad 2000; 46:343–368.

62 Giannantonio DJ, Kurth JC, Kurtis KE, Sobecky PA. Effects of concrete properties and nutrients on fungal colonization and fouling. Int Biodeterior Biodegrad 2009; 63:252–259.

63 Gaylarde C, Silva MR, Warscheid T. Microbial impact on building materials: an overview. Mater Struct 2003; 36:342–352.